Joint Diseases and Related Surgery

Jt Dis Relat Surg
2026;37(2):306-313

ORIGINAL ARTICLE

Patient-specific 3D printed guides for repairing posterior root tears of the medial meniscus: A cadaveric study

María Durán-Serrano, MD[1,6], Ignacio Colom-Diaz, MD[2], Antonio-Francisco Laclériga-Giménez, PhD[3], Daniel Delfau-Lafuente, MD[4], Adrián Roche-Albero, PhD[1,5,6], Miguel Lizcano-Palomares, MD[1,3], Carlos Martín-Hernández, PhD[1,5]

[1]Orthopedic and Trauma Surgery Service, Miguel Servet University Hospital, Zaragoza, Spain
[2]Younext/podoactiva, Institute for Advanced Orthopedic Research, Huesca, Spain
[3]Orthopedic and Trauma Surgery Service, Viamed Montecanal Hospital, Zaragoza, Spain
[4]General Surgery Service, Alcañiz Hospital, Alcañiz (Teruel), Spain
[5]Orthopedic and Trauma Surgery Service, Instituto Investigación Sanitaria Aragón (IIS Aragón), Zaragoza, Spain
[6]University of Zaragoza, Zaragoza, Spain

Meniscal root tears, classified as radial tears or avulsions up to 1 cm from the meniscal insertion, disrupt the circumferential fibers that convert axial loads into hoop stresses.[1] Medial posterior root tears reproduce the biomechanical consequences of total meniscectomy with increased contact pressure, reduced contact area, and higher risk of early osteoarthritis.[2-6] They are found in 7 to 9% of knee arthroscopies, mostly in the medial compartment, and their timely recognition is crucial, as delayed diagnosis or inadequate repair compromise joint

Received: February 26, 2025
Accepted: October 03, 2025
Published online: November 04, 2025

Correspondence: María Durán-Serrano, MD. Orthopedic and Trauma Surgery Service, Miguel Servet University Hospital, 50009 Zaragoza, Spain.

E-mail: mdurans@salud.aragon.es

Citation: Durán-Serrano M, Colom-Diaz I, Laclériga-Giménez AF, Delfau-Lafuente D, Roche-Albero A, Lizcano-Palomares M, Martín-Hernández C. Patient-specific 3D printed guides for repairing posterior root tears of the medial meniscus: A cadaveric study. Jt Dis Relat Surg 2026;37(2):306-313. doi: 10.52312/jdrs.2026.2233.

© 2026 Joint Diseases and Related Surgery. This is an open access article published under the terms of the Creative Commons Attribution-NonCommercial 4.0 International License (CC BY-NC 4.0), which permits non-commercial use, distribution, reproduction, and adaptation in any medium, provided the original work is properly cited. http://creativecommons.org/licenses/by-nc/4.0/

ABSTRACT

Objectives: The aim of this study was to evaluate the accuracy of tibial tunnel placement using patient-specific three-dimensional (3D)-printed guides for repairing medial meniscus posterior root tears designed from magnetic resonance imaging (MRI) scans.

Materials and methods: Five right fresh-frozen cadaveric knees underwent MRI scanning with 1-mm isotropic slices. For each specimen, custom guides were created to generate two transosseous tibial tunnels, with design based on anatomical landmarks including the medial tibial eminence (MTE) and the posterior cruciate ligament (PCL) insertion. Guide design was done using Rhinoceros software, segmentation of bone structures and soft tissues in 3D Slicer, and printing in polyamide. After arthroscopic repair, computed tomography scans and anatomical dissections were performed to measure the accuracy of tunnel placement relative to the native medial meniscus posterior root attachment (MMPRA), the MTE, and the PCL. Individual pre- and postoperative measurements were compared to verify anatomical accuracy, and pooled data from all knees were analyzed.

Results: Individual evaluation showed minimal differences between pre- and postoperative measurements, ranging from 0.00 to 0.09 mm. Pooled analysis revealed no significant differences in the measurements taken: PCL-MMPRA (p = 0.313), MTE-MMPRA (p = 0.705) or the width of MMPRA (p = 0.125). The guides enabled precise and reproducible tunnel placement, with consistent targeting of the anatomical footprint. Each guide cost approximately €30, with a production turnaround time of less than one week.

Conclusion: Patient-specific 3D-printed guides enable the effective creation of two anatomically accurate tibial tunnels for medial meniscus posterior root repair. This approach offers a rapid and precise solution for anatomical restoration using MRI-guided planning.

Keywords: Additive manufacturing, knee arthroscopy, knee customized guides, meniscus posterior root tears repair, patient-specific instrument, 3D printing.

preservation.[7,8] Conservative treatment is reserved for patients with advanced cartilage degeneration (Kellgren-Lawrence Grade 3-4), advanced age, obesity, or significant comorbidities.[3,9,10]

Anatomical repair via transtibial tunnel techniques has become the gold standard surgical technique.[9] However, creating tibial tunnels that exit precisely at the native meniscal footprint still remains technically demanding. Existing surgical guides do not permit patient-specific planning, lack compatibility with variable tibial anatomy, and may result in malpositioned tunnels due to obstacles such as the tibial spines or femoral condyles. Misplacement has been linked to poor functional outcomes and rapid osteoarthritis progression.[11]

Three-dimensional (3D) printing has increasingly been used in orthopedic surgery to produce custom instrumentation for fracture fixation, oncology orthopedic reconstructions, osteotomies and arthroplasty.[12-19] However, no applications to date have addressed meniscal root repair with patient-specific guides. This represents a significant gap in the field, as tailored guides could improve surgical accuracy and reproducibility in this technically demanding procedure.

Although the main clinical challenge is the clear lack of individualized instruments for ensuring anatomical tunnel placement during medial meniscus posterior root repairs, in the present study, we aimed to evaluate the anatomical accuracy of tibial tunnels created using magnetic resonance imaging (MRI)-based, patient-specific 3D-printed guides designed to restore the medial meniscus posterior root via two transtibial tunnels.

MATERIALS AND METHODS

This single-center, cadaveric study was conducted at University of Zaragoza (Spain), Department of Anatomy between December 2022 and December 2024. The study protocol was approved by the Aragón Ethics Committee (Date: 14.12.2022, No: PI22/529 TA).

In this study, we developed a cadaveric study in five right knees. Five right fresh-frozen cadaveric knee specimens with no evidence of prior injury, previous surgery, osteoarthritis, meniscal pathology, or ligament pathology were used. The cadaveric samples used in this study were obtained from a tissue bank and designated for medical research purposes. All specimens were kept at –20°C and thawed for 24 h prior to preparation.

Preoperative images and segmentation

Each specimen underwent MRI using a Magnetom Sola scanner (Siemens Healthineers, Munich, Germany) with 1-mm isotropic slice thickness and interval. This resolution provided adequate voxel uniformity (x = y = z), enabling 3D reconstruction. Images were exported as Digital Imaging and Communications in Medicine (DICOM) files and processed in 3D Slicer version 5.2 software (The Slicer Community, MA, USA), using semi-automatic segmentation for bone structures.[20] Although 3D Slicer lacks automated tools for soft tissue segmentation from MRI, experienced users manually delineated structures such as the meniscus and posterior cruciate ligament (PCL) (Figure 1).

The anatomical landmarks identified for guide planning included:

- The native footprint of the medial meniscus posterior root attachment (MMPRA)
- The apex of the medial tibial eminence (MTE)
- The most superior tibial attachment of the PCL.

The coordinates of the MMPRA footprint were defined in three-dimensional space (x, y, z), referenced from MTE and PCL. These coordinates were used for designing each guide.

Guide design and manufacturing

A single customized guide was designed per knee using Rhinoceros CAD software (Rhino, Washington DC, USA). Each guide included a defined entry point on the anteromedial tibial cortex and two 3-mm bores to guide the creation of two parallel tibial tunnels converging at the MMPRA footprint (Figure 2). Tunnel exits were planned using the MRI-based 3D coordinates of the target footprint.

To assess tunnel orientation, three variants of the guide were virtually created per knee with angles of 30°, 45°, and 60°, modifying only the external guide arm orientation (Figure 3). Although tunnel angles are largely defined by the external anatomy, this step ensured the selection of a configuration that avoided intra-articular impingement and optimized tunnel length and placement. After virtual evaluation, the 60° guide was selected for all specimens because 30° and 45° guides created short and horizontal tunnels.

All guides were printed in sterilizable polyamide (Figure 4) using an HP Jet Fusion 5200 printer (HP, CA, USA). Production cost was €30 per guide.

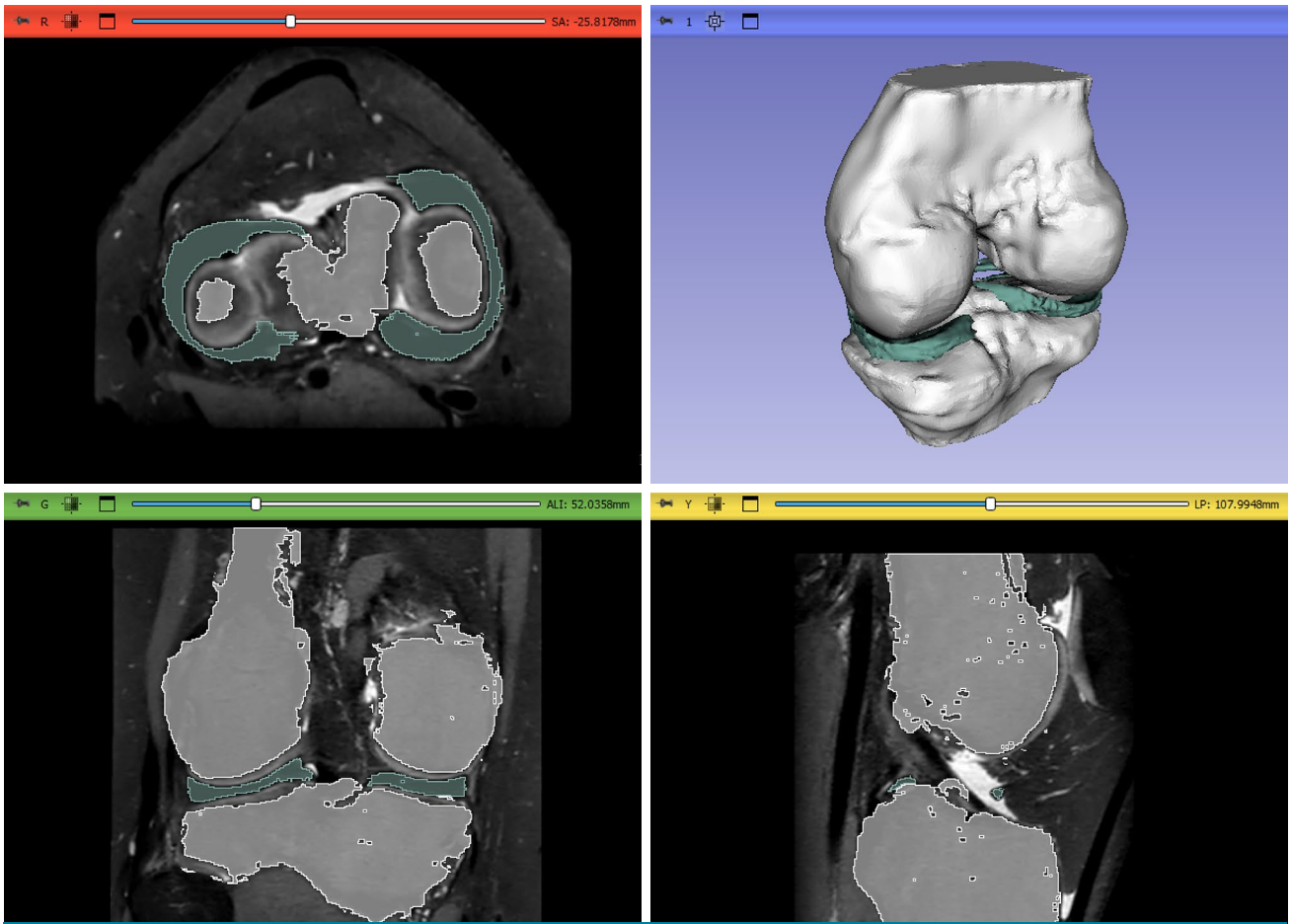


FIGURE 1. Segmentation process in 3D Slicer. Axial, coronal, and sagittal MRI views of the knee with 3D virtual reconstruction.
3D, three-dimensional; MRI, magnetic resonance imaging.

Manufacturing time from MRI acquisition to printed model was less than one week.

Surgical procedure

Each procedure was performed with the specimen in the supine position and the knee flexed to 90°. Standard anterolateral and anteromedial portals were used for arthroscopy (Figure 5). The posterior horn of the medial meniscus was arthroscopically detached, and the 60° patient-specific guide was fixed on the anteromedial tibia. Two 2.7-mm tunnels were drilled, via the personalized guide, with an Acufex® trephine over a Kirschner wire. The target for tunnel exit was the MMPRA footprint, located posterior to the apex of the MTE and anteromedial to the tibial attachment of the PCL (Figure 6).

Postoperative evaluation

All specimens underwent computed tomography (CT) examination after surgery. The CT images were obtained with an Aquilion™ 64 CT System (Toshiba Medical Systems, Tochigi, Japan) using 1-mm slice thickness.

Tunnel positions were analyzed in coronal, axial, and sagittal planes. The following parameters were measured (Figure 7):

- Distance from MTE apex to the midpoint between tunnel exits
- Distance from this midpoint to the most superior tibial attachment of the PCL
- Reinsertion width, calculated as the linear distance between both tunnels, including their full diameter.

All measurements were performed twice, and the mean values were recorded.

Subsequently, anatomical dissection was performed to directly visualize tunnel positioning relative to the PCL attachment. Digital calipers

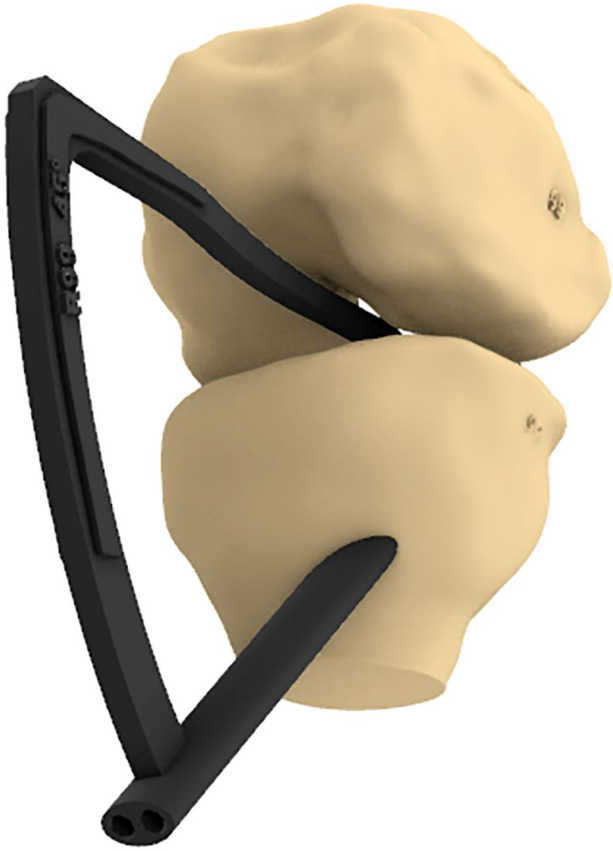


FIGURE 2. Virtual 3D reconstruction of a cadaveric knee with digitally planned customized guide.
3D, three-dimensional.

(accuracy: 0.02 mm; resolution: 0.01 mm; UNE-EN ISO/IEC 17025 compliant) were used. All measurements were expressed in mm.

Statistical analysis

Two complementary approaches were used to analyze the data. Firstly, each specimen was assessed individually by directly comparing its pre- and postoperative values for all anatomical references. This descriptive comparison allowed us to assess whether the surgical technique reproduced the anatomical footprint in each specimen. Secondly, to provide a formal statistical evaluation, all paired data were pooled and analyzed using the Wilcoxon signed-rank test, a non-parametric method appropriate for small sample sizes (n = 5) and paired observations. Statistical analysis was performed using the Python version 3.11 software (Python Software Foundation, Wilmington, DE, USA) with the SciPy version 1.11 library. A p value of < 0.05 was considered statistically significant.

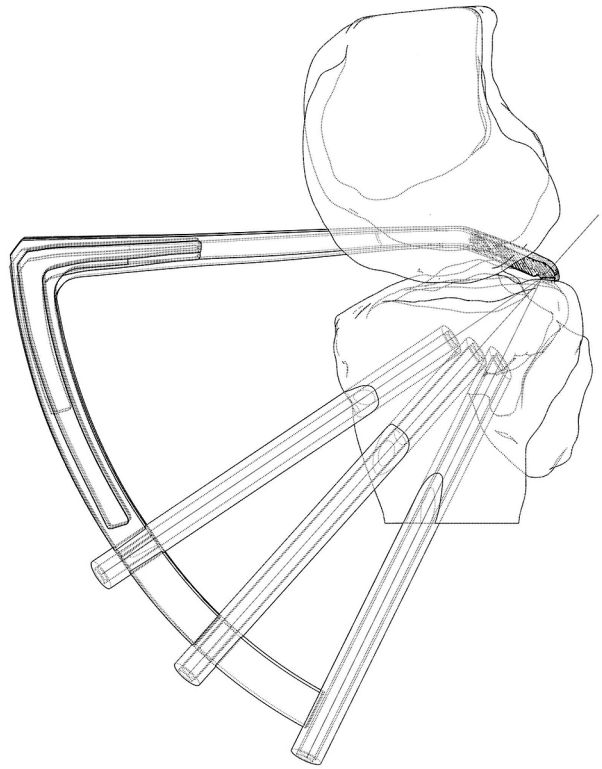


FIGURE 3. Comparison of tunnel angles (30°, 45°, 60°) for guide optimization, based on 3D knee model.
3D, three-dimensional.

RESULTS

A total of five cadaveric knees were evaluated in this study. Measurements of the anatomical references were obtained pre- and postoperatively (Table I).

The accuracy of tunnel placement was evaluated by comparing the postoperative position of the tibial tunnel exits with the preoperatively planned coordinates derived from MRI (Table I).

Based on individual evaluation, the five knees showed almost identical values before and after the surgical procedure. The observed differences ranged between 0.00 and 0.09 mm (Table I), and none of them could be regarded as clinically relevant.

Based on pooled analysis of all specimens, no statistically significant differences were observed in PCL-MMPRA ($p = 0.313$), MTE-MMPRA ($p = 0.705$), or MMPRA reinsertion width ($p = 0.125$). No significant differences were found in the statistical analysis between pre- and postoperative measurements for any of the three parameters evaluated.



FIGURE 4. Final printed patient-specific guide in polyamide.



FIGURE 5. Arthroscopic placement of guide.

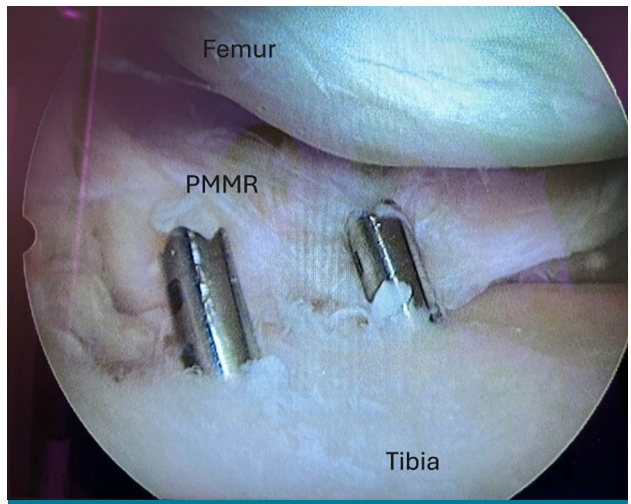


FIGURE 6. Tunnel drilling under direct visualization with 2.7-mm cannulated drills.
PMMR, posterior medial meniscus root.

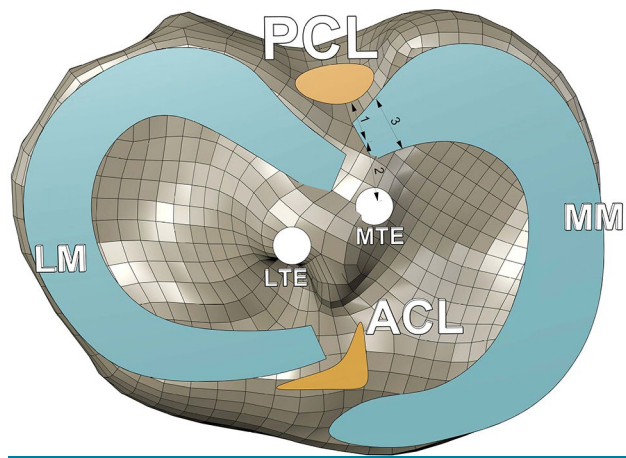


FIGURE 7. Schematic of planned tunnel positions and anatomical landmarks.
PCL, posterior cruciate ligament; LM, lateral meniscus; LTE, lateral tibial eminence; MTE, medial tibial eminence; ACL, anterior cruciate ligament, MM, medial meniscus. 1: distance from the midpoint of the MM insertion to the most superior tibial attachment of the PCL. 2: distance from MTE apex to the midpoint of the MM insertion. 3: insertion width of MM posterior root.

Taken together, both the individual comparisons and the pooled statistical test indicated that the technique restored the meniscal root to its anatomical position with high anatomical accuracy.

Across all specimens, the tunnel exits were visually confirmed to lie posterior to the apex of the MTE and anteromedial to the tibial PCL insertion, consistent with established anatomical descriptions.

TABLE I
Pre- and postoperative anatomical measurements

Knee ID	Parameter	Preoperative (mm)	Postoperative (mm)	Difference (Post-Pre), (mm)
1	PCL-MMPRA	8.06	8.02	–0.04
	MTE-MMPRA	11.64	11.65	+0.01
	Reinsertion width	10.22	10.29	+0.07
2	PCL-MMPRA	8.55	8.52	–0.03
	MTE-MMPRA	11.82	11.84	+0.02
	Reinsertion width	10.61	10.70	+0.09
3	PCL-MMPRA	8.70	8.72	+0.02
	MTE-MMPRA	12.06	12.06	0.00
	Reinsertion width	10.71	10.70	–0.01
4	PCL-MMPRA	7.88	7.85	–0.03
	MTE-MMPRA	11.26	11.24	–0.02
	Reinsertion width	10.34	10.38	+0.04
5	PCL-MMPRA	8.75	8.76	+0.01
	MTE-MMPRA	12.32	12.30	–0.02
	Reinsertion width	10.92	10.99	+0.07

PCL, posterior cruciate ligament; MMPRA, medial meniscus posterior root attachment; MTE, medial tibial eminence; PCL-MMPRA, distance from the most superior tibial attachment of the PCL to the midpoint between tunnel exits. MTE-MMPRA: distance from MTE apex to the midpoint between tunnel exits. Reinsertion width, calculated as the linear distance between both tunnels, including their full diameter

Post-dissection assessment confirmed these positions, and no tunnel exit was observed to deviate outside the intended anatomical region.

The reinsertion width varied slightly among specimens, ranging from 10.29 to 10.99 mm, indicating the practical outcome of guide accuracy in replicating a broad-based contact area for meniscal healing. While this was not a direct surrogate for biological fixation strength, consistent spacing supported reproducibility in guide use.

DISCUSSION

In this cadaveric study, we evaluated the anatomical accuracy of tibial tunnels created using MRI-based, patient-specific 3D-printed guides designed to restore the medial meniscus posterior root via two transtibial tunnels. Our study results demonstrated the feasibility of MRI-based, patient-specific 3D-printed guides for medial meniscus posterior root repair. In all cadaveric specimens, the guides enabled accurate and reproducible creation of two tibial tunnels directed to the anatomical root footprint, confirming their technical viability.

Unlike most patient-specific instrumentation that relies on CT for bone segmentation, this approach shows that high-resolution MRI can provide sufficient detail for guide design, avoiding additional imaging.[15,18] Tunnel positioning was accurate, with exit points consistent with prior anatomical descriptions.[9,11,21] This accuracy is critical, as improper tunnel placement compromises meniscal function and increases the risk of PCL injury.[21]

Meniscal root tears alter tibiofemoral biomechanics, increasing contact pressure and reducing contact area.[3,4,9,22] Anatomical repair has been shown to restore biomechanics and improve joint loading.[3,9,23-26] The transtibial pullout repair, particularly the anatomical two-tunnel variation, is considered the gold standard.[2,3,9,10,22,27] Our guides were specifically developed to facilitate this technique, offering a practical single-device solution for double tunnel creation.

Compared to conventional guides, 3D-printed instruments offer customization, cost-effectiveness, and usability in cases with challenging anatomy or limited availability of commercial devices. While MRI-based design is more demanding than CT processing, it aligns with routine diagnostic practice and allows better identification of meniscal root attachments. The CT is still used postoperatively for tunnel verification, complemented by cadaveric dissection to assess PCL relationships. Overall, MRI-based 3D-printed guides represent a promising tool to improve accuracy, reproducibility, and accessibility in meniscal root repair, warranting further biomechanical and clinical validation.

Nonetheless, this study has several limitations. This study was conducted on cadaveric specimens without previous knee injuries. A relevant limitation, however, is that MRI was obtained from intact knees, and the lesion was artificially created afterwards, which may not fully replicate the clinical scenario of naturally occurring injuries. The sample size was also relatively small due to the high cost of every specimen and every image test, which limits the generalizability of the results. In addition, custom-made guides were designed from MRI images. Finally, all surgical procedures were performed by a single surgeon.

In conclusion, MRI-based, patient-specific 3D-printed guides provide a rapid and anatomically accurate method for double tibial tunnel creation in MMPRA repair. These findings support technical feasibility, reproducibility, and individualized anatomical adaptation, offering a solid basis for future clinical translation and further investigation into patient-specific instrumentation for soft-tissue knee surgery.

Data Sharing Statement: The data that support the findings of this study are available from the corresponding author upon reasonable request.

Author Contributions: C.M.H.: Idea/concept; C.M.H., M.D.S.: Design, writing the article; A.R.A., A.F.L.G.: Control/supervision; C.M.H., M.D.S., I.C.D.: Data collection and/or processing, analysis and/or interpretation; M.D.S., M.L.P., D.D.L.: Literature review; A.R.A., M.L.P., D.D.L., A.F.L.G., I.C.D.: Critical review.

Conflict of Interest: The authors declared no conflicts of interest with respect to the authorship and/or publication of this article.

Funding: This study received funding from the Spanish Arthroscopy Association.

AI Disclosure: The authors declare that artificial intelligence (AI) tools were not used, or were used solely for language editing, and had no role in data analysis, interpretation, or the formulation of conclusions. All scientific content, data interpretation, and conclusions are the sole responsibility of the authors. The authors further confirm that AI tools were not used to generate, fabricate, or 'hallucinate' references, and that all references have been carefully verified for accuracy.

REFERENCES

1. Koenig JH, Ranawat AS, Umans HR, Difelice GS. Meniscal root tears: Diagnosis and treatment. Arthroscopy 2009;25:1025-32. doi: 10.1016/j.arthro.2009.03.015.
2. Bhatia S, LaPrade CM, Ellman MB, LaPrade RF. Meniscal root tears: Significance, diagnosis, and treatment. Am J Sports Med 2014;42:3016-30. doi: 10.1177/0363546514524162.
3. Hantouly AT, Aminake G, Khan AS, Ayyan M, Olory B, Zikria B, et al. Meniscus root tears: State of the art. Int Orthop 2024;48:955-64. doi: 10.1007/s00264-024-06092-w.
4. Allaire R, Muriuki M, Gilbertson L, Harner CD. Biomechanical consequences of a tear of the posterior root of the medial meniscus. Similar to total meniscectomy. J Bone Joint Surg Am 2008;90:1922-31. doi: 10.2106/JBJS.G.00748.
5. LaPrade CM, Jansson KS, Dornan G, Smith SD, Wijdicks CA, LaPrade RF. Altered tibiofemoral contact mechanics due to lateral meniscus posterior horn root avulsions and radial tears can be restored with in situ pull-out suture repairs. J Bone Joint Surg Am 2014;96:471-9. doi: 10.2106/JBJS.L.01252.
6. Marzo JM, Gurske-DePerio J. Effects of medial meniscus posterior horn avulsion and repair on tibiofemoral contact area and peak contact pressure with clinical implications. Am J Sports Med 2009;37:124-9. doi: 10.1177/0363546508323254.
7. LaPrade RF, Ho CP, James E, Crespo B, LaPrade CM, Matheny LM. Diagnostic accuracy of 3.0 T magnetic resonance imaging for the detection of meniscus posterior root pathology. Knee Surg Sports Traumatol Arthrosc 2015;23:152-7. doi: 10.1007/s00167-014-3395-5.
8. Matheny LM, Ockuly AC, Steadman JR, LaPrade RF. Posterior meniscus root tears: Associated pathologies to assist as diagnostic tools. Knee Surg Sports Traumatol Arthrosc 2015;23:3127-31. doi: 10.1007/s00167-014-3073-7.
9. Monson JK, LaPrade RF. Posterior medial meniscus root tears: Clinical implications, surgical management, and post-operative rehabilitation considerations. Int J Sports Phys Ther 2025;20:127-36. doi: 10.26603/001c.126967.
10. LaPrade RF, Floyd ER, Carlson GB, Moatshe G, Chahla J, Monson JK. Meniscal root tears: solving the silent epidemic. J Am Acad Sports Med 2021;2:47-57.
11. Floyd ER, Rodriguez AN, Falaas KL, Carlson GB, Chahla J, Geeslin AG, et al. The natural history of medial meniscal root tears: A biomechanical and clinical case perspective. Front Bioeng Biotechnol 2021;9:744065. doi: 10.3389/fbioe.2021.744065.
12. Shen Z, Wang H, Duan Y, Wang J, Wang F. Application of 3D printed osteotomy guide plate-assisted total knee arthroplasty in treatment of valgus knee deformity. J Orthop Surg Res 2019;14:327. doi: 10.1186/s13018-019-1349-9.
13. Hooper J, Schwarzkopf R, Fernandez E, Buckland A, Werner J, Einhorn T, et al. Feasibility of single-use 3D-printed instruments for total knee arthroplasty. Bone Joint J 2019;101-B:115-20. doi: 10.1302/0301-620X.101B7.BJJ-2018-1506.R1.

14. Rankin I, Rehman H, Frame M. 3D-printed patient-specific ACL femoral tunnel guide from MRI. Open Orthop J 2018;12:59-68. doi: 10.2174/1874325001812010059.
15. Bahadır B, Atik OŞ, Kanatlı U, Sarıkaya B. A brief introduction to medical image processing, designing and 3D printing for orthopedic surgeons. Jt Dis Relat Surg 2023;34:451-4. doi: 10.52312/jdrs.2023.57912.
16. Zhang H, Liu Y, Dong Q, Guan J, Zhou J. Novel 3D printed integral customized acetabular prosthesis for anatomical rotation center restoration in hip arthroplasty for developmental dysplasia of the hip crowe type III: A Case Report. Medicine (Baltimore) 2020;99:e22578. doi: 10.1097/MD.0000000000022578.
17. McCulloch RA, Frisoni T, Kurunskal V, Maria Donati D, Jeys L. Computer navigation and 3D printing in the surgical management of bone sarcoma. Cells 2021;10:195. doi: 10.3390/cells10020195.
18. Si C, Bai B, Cong W, Zhang L, Guan R. Efficacy of 3D printing-assisted treatment for acetabular fractures. Jt Dis Relat Surg 2024;35:521-8. doi: 10.52312/jdrs.2024.1756.
19. González-Alonso M, Hermida-Sánchez M, Martínez-Seijas P, Ruano-Ravina A. Application of 3D printing in the treatment of appendicular skeleton fractures: Systematic review and meta-analysis. J Orthop Res 2021;39:2083-92. doi: 10.1002/jor.24939.
20. Toranzo-Benítez J. Procesamiento de imágenes radiológicas mediante 3D Slicer. [Trabajo de fin de Grado] Salamanca: Universidad de Salamanca; 2024.
21. Johannsen AM, Civitarese DM, Padalecki JR, Goldsmith MT, Wijdicks CA, LaPrade RF. Qualitative and quantitative anatomic analysis of the posterior root attachments of the medial and lateral menisci. Am J Sports Med 2012;40:2342-7. doi: 10.1177/0363546512457642.
22. Padalecki JR, Jansson KS, Smith SD, Dornan GJ, Pierce CM, Wijdicks CA, et al. Biomechanical consequences of a complete radial tear adjacent to the medial meniscus posterior root attachment site: In situ pull-out repair restores derangement of joint mechanics. Am J Sports Med 2014;42:699-707. doi: 10.1177/0363546513499314.
23. LaPrade CM, LaPrade MD, Turnbull TL, Wijdicks CA, LaPrade RF. Biomechanical evaluation of the transtibial pull-out technique for posterior medial meniscal root repairs using 1 and 2 transtibial bone tunnels. Am J Sports Med 2015;43:899-904. doi: 10.1177/0363546514563278.
24. Moatshe G, Chahla J, Slette E, Engebretsen L, Laprade RF. Posterior meniscal root injuries. Acta Orthop 2016;87:452-8. doi: 10.1080/17453674.2016.1202945.
25. Stärke C, Kopf S, Gröbel KH, Becker R. The effect of a nonanatomic repair of the meniscal horn attachment on meniscal tension: A biomechanical study. Arthroscopy 2010;26:358-65. doi: 10.1016/j.arthro.2009.08.013.
26. Ahn JH, Jeong HJ, Lee YS, Park JH, Lee JW, Park JH, et al. Comparison between conservative treatment and arthroscopic pull-out repair of the medial meniscus root tear and analysis of prognostic factors for the determination of repair indication. Arch Orthop Trauma Surg 2015;135:1265-76. doi: 10.1007/s00402-015-2269-8.
27. Pangaud C, Rarchaert M, Belgaid V, Ollivier M, Fessy MH, Viste A. An anatomical study of the meniscal roots of the knee: Landmarks for its surgical reconstruction and implications for knee surgeons. Surg Radiol Anat 2022;44:971-7. doi: 10.1007/s00276-022-02979-8.